Perioperative Precision Medicine
ISSN: 2957-5443

Zentime

Review Article https://doi.org/10.61189/251934gxqfic

Diagnostic performance of deep learning for brachial plexus ultrasound: A systematic review

Jiaen Wu[1], Jiaxun Jiang[1], Zhaopeng Zhou[1], Miao Zhou[2], Liangqing Lin[3], Jinjing Wu[1], Haipo Cui[1]

[1]School of Health Science and Engineering, University of Shanghai for Science and Technology, Shanghai 200093, China. [2]Jiangsu Cancer Hospital, Changzhou 213164, Jiangsu Province, China. [3]Department of Anesthesiology, The First Hospital of Putian, Putian 351100, Fujian, China.

Corresponding author: Haipo Cui.

Declaration of conflict of interest: None.

Received April 9, 2025; Accepted August 13, 2025; Published December 31, 2025

Highlights

- This study compares deep learning methods for brachial plexus ultrasound segmentation, demonstrating improved segmentation efficiency and reduced learning difficulty, which may enhance perioperative regional anesthesia planning and safety.
- U-Net is favored for brachial plexus segmentation due to its enhanced ability to capture contextual features through increased channel utilization.
- Available public brachial plexus datasets are summarized, offering valuable resources for future research and perioperative ultrasound applications.

Abstract

Ultrasound-guided nerve block is a safe and effective regional anesthesia technique; however, accurate identification of the brachial plexus remains challenging due to its small size and low contrast in ultrasound images. Recent advances in deep learning offer promising solutions to enhance brachial plexus segmentation and improve perioperative regional anesthesia precision and safety. This review systematically summarizes current deep learning approaches applied to ultrasound-based brachial plexus segmentation. We highlight key models, including Convolutional Neural Networks, the U-shaped Convolutional Neural Networks and their variants, Mask Region-Based Convolutional Neural Networks, and Generative Adversarial Network-based architectures, and compare their reported performances, with Dice Similarity Coefficients ranging from 0.5865 to 0.882 and Intersection over Union values up to 0.6957. Among them, U-Net remains the most frequently employed due to its balance of accuracy and computational efficiency. Moreover, novel models such as multi-objective brachial plexus segmentation network and BPMSegNet have demonstrated superior segmentation performance by incorporating attention mechanisms and spatial contrast features. Notwithstanding these advancements, challenges persist, particularly limited dataset availability and insufficient model generalization. This review provides a comprehensive overview of recent progress, evaluates comparative performance metrics, and outlines future directions to improve model robustness and clinical applicability and clinical applicability in the perioperative setting.

Keywords: Deep learning, brachial plexus, image segmentation

Introduction

The brachial plexus is a complex network of nerves originating from the anterior rami of cervical and upper thoracic spinal nerves, responsible for the motor and sensory functions of the upper limbs [1]. Injuries to the brachial plexus may result in sensory deficits, neuropathic pain, or even paralysis, significantly diminishing patients' quality of life [2, 3]. Traditional treat-

Address correspondence to: Haipo Cui, School of Health Science and Engineering, University of Shanghai for Science and Technology, No. 516 Jungong Road, Yangpu District, Shanghai 200093, China. E-mail: h_b_cui@163.com.

ment approaches, including pharmacologic analgesia, physiotherapy, and surgical nerve repair, are limited by challenges such as imprecise localization, slow recovery, and significant side effects [3, 4].

Ultrasound-guided brachial plexus block has gained popularity due to its safety, real-time imaging capabilities, and radiation-free operation [5, 6]. Compared with CT or MRI, ultrasound is particularly suitable for bedside procedures and repeated interventions, making it a preferred choice in perioperative regional anesthesia and pain management [7]. However, clinical success relies heavily on operator expertise and precise identification of the low-contrast, small-diameter brachial plexus structures within noisy ultrasound images [8, 9].

In recent years, deep learning, a subfield of artificial intelligence, has revolutionized medical image analysis. Unlike traditional machine learning methods based on hand-crafted features, deep learning leverages multilayer neural networks to automatically learns hierarchical representations from raw data [10]. Notably, Convolutional Neural Networks (CNNs) have demonstrated superior performance in extracting spatial features and patterns in medical images. Architectures such as U-shaped Convolutional Neural Networks (U-Net) and Residual Networks (ResNet) have been widely used for tasks such as organ segmentation, tumor detection, and nerve identification [10, 11]. In ultrasound brachial plexus imaging, improved deep learning models have achieved encouraging outcomes; for instance, U-Net variants have reported Dice coefficients up to 0.658, while modified SegNet models have achieved 96% segmentation accuracy [11, 12].

Despite these advances, challenges persist, including ultrasound image artifacts, anatomical variability, and the scarcity of publicly available datasets. Therefore, a systematic review of current deep learning approaches is essential to guide future developments.

This paper provides a comprehensive review of deep learning applications in brachial plexus segmentation from ultrasound images. We summarize commonly used public datasets, evaluate representative deep learning architectures, and compare model performance using metrics such as Dice coefficient and Intersection over Union (IoU). In addition, current challenges and future directions are discussed. This work aims to provide researchers and clinicians with an informed perspective on the potential and constraints of AI-assisted nerve segmentation. In particular, accurate and automated brachial plexus segmentation can enhance perioperative ultrasound-guided nerve block precision, reduce block failure rates, minimize complications, shorten procedural times, and ultimately improve patient safety and outcomes in upper limb surgeries.

Data and preprocessing

Dataset

High-quality datasets are fundamental for training deep learning models, as they directly determine model accuracy and generalizability. When selecting datasets, not only the size and volume of data but also its diversity and quality should be considered. However, in medical image processing, many datasets remain inaccessible due to patient privacy concerns, which limits the availability of high-quality training data. Fortunately, some researchers and academic competitions have released publicly available datasets. For example, the Ultrasound Nerve Segmentation competition held in mid-2016 focused on identifying brachial plexus nerve structures [13]. **Table 1** summarizes the currently available public ultrasound datasets containing brachial plexus images.

Dataset preprocessing

Although large-scale image datasets can yield satisfactory results in model training, such ideal conditions are rarely achievable in practice. This limitation can be improved through image preprocessing, which effectively enhances the accuracy and performance of deep learning models [16]. Common preprocessing steps include denoising, normalization, and image registration, all of which reduce noise and ensure data consistency [17]. For example, Ly *et al.* applied image rotation to increase sample size and enhance model generalization, while Wang *et al.* employed random cropping and scaling, which were shown to be critical for successful model training [18, 19]. **Table 2** summarizes the preprocessing methods reported in the literature.

Table 1. Medical image dataset

Datasets	Image types	Position	Sample size	Data collection methods	Annotation quality
Ultrasound nerve segmentation	Ultrasonic	Brachial plexus	16780	Details not provided	Expert-trained annotators
Brachial-plexus-segmentation	Ultrasonic	Supraclavicular region	500	Two hospitals not mentioned	Expert-labeled, double-checked
UBPD [14]	Ultrasonic	Brachial plexus	1052	SIEMENS ACUSON NX3 Elite and Philips EPIQ5	Professional anesthesiologists
FLUID-sensitive dataset [15]	MRI	Brachial plexus	274	Standard MRI protocols	Radiologist

Table 2. Preprocessing methods

Reference	Datasets	Preprocessing methods
Wang *et al.* [19]	Kaggle	Random rotation/scaling/shear
Wang *et al.* [20]	Kaggle	Median filtering
Ding *et al.* [14]	UBPD	Bilinear interpolation

Overview of deep learning

The typical workflow for deep learning–based brachial plexus segmentation comprises five stages: (1) dataset preparation, involving the collection and annotation of brachial plexus ultrasound images; (2) image preprocessing, including denoising, normalization, augmentation, and cropping; (3) model selection and training, in which architectures such as CNN and U-Net are applied to extract and learn image features; (4) segmentation inference, in which the trained model is used to segment new images; and (5) performance evaluation, assessing model effectiveness using established metrics. This workflow is illustrated in **Figure 1**, which outlines the end-to-end process from data acquisition to model evaluation. It enables automated and accurate identification of brachial plexus structures, supporting clinical applications such as ultrasound-guided nerve blocks.

CNNs

CNNs are deep learning models particularly effective for image analysis and have been widely applied across various fields. Their core principle lies in hierarchical feature abstraction, progressively extracting feature from low-level texture to high-level semantics representations [21]. The workflow is shown in **Figure 2**.

First, the convolution layer applies filters to the input image to generate feature maps through convolution operations, with different convolution layers capturing different feature levels. The resulting outputs are processed by an activation function, most commonly the Rectified Linear Unit, which introduces nonlinearity and enables the network to learn more complex patterns [22]. Then, the pooling layer down-samples the feature maps to reduce data dimensionality and calculational cost. Finally, the fully connected layer integrates all the features from previous layers and produces the final output through linear transformation and activation.

The advantage of CNN is that it can automatically learn image features, offering greater efficiency than traditional manual feature extraction. Parameter sharing of convolution kernel at different positions reduces the number of model parameters and improves training efficiency. In addition, through convolution and pooling operations, CNN confers certain translation, rotation, and scale invariance, contributing to their robustness. These characteristics have led to remarkable success in tasks such as image classification, target detection, and medical image segmentation.

Classic architectures such as LeNet and GoogLeNet are foundational CNN models, and many modern networks build upon these designs [23, 24]. CNN can also be integrated with other models to enhance accuracy. For instance, Boxtel JV *et al.* employed CNN as a classifier to identify brachial plexus regions in neck ultrasound images, followed by U-Net for segmentation, achieving superior performance compared with the original segmentation model [25].

Mask region-based CNN (R-CNN)

Mask R-CNN is a deep learning model for instance segmentation, achieving pixel-level

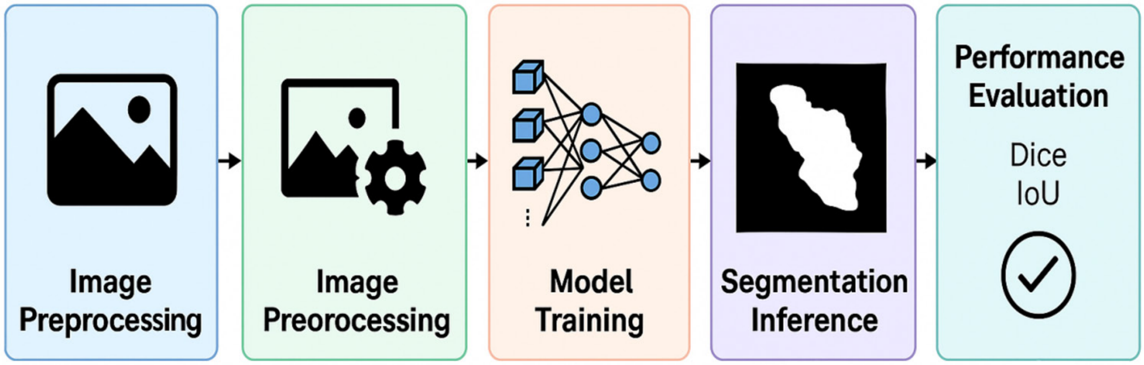

Figure 1. General workflow of deep learning.

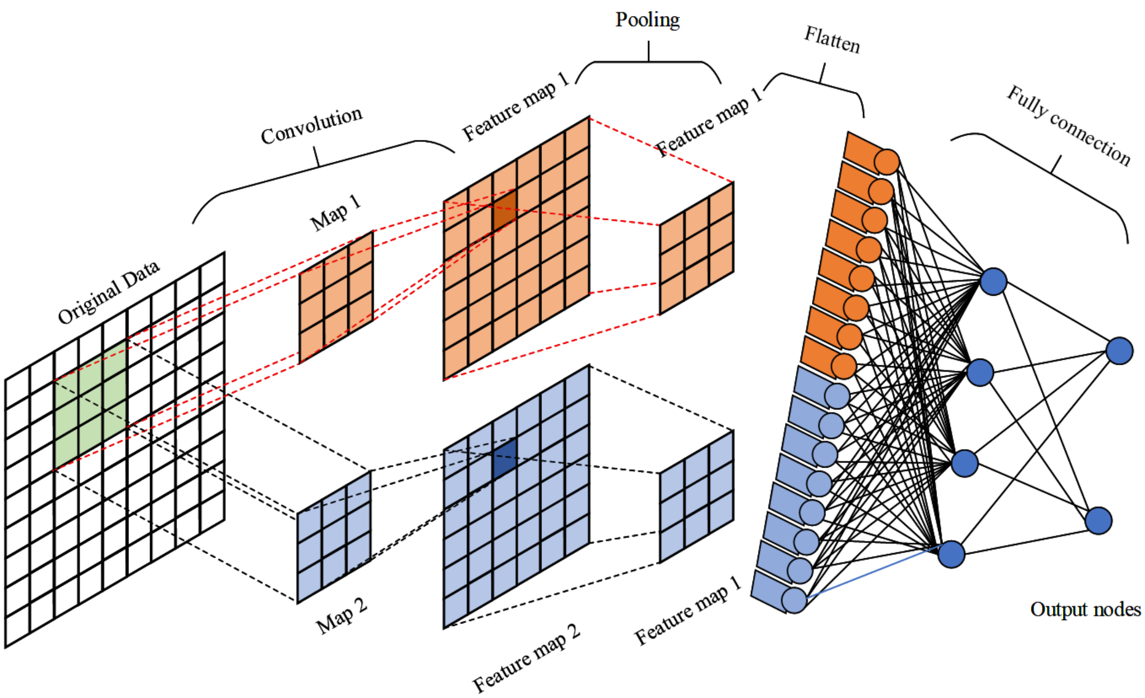

Figure 2. Schematic diagram of convolutional neural network.

accuracy by simultaneously identifying and segmenting individual objects in an image [26]. It extends Faster R-CNN by introducing an additional branch for object mask prediction, thereby enabling instance segmentation alongside target detection. **Figure 3** shows the network structure of Mask R-CNN.

The Mask R-CNN workflow starts with an input image, from which a CNN backbone extracts multi-level feature maps. Then, the Feature Pyramid Network processes these feature maps to construct a multi-scale feature pyramid, allowing the model to detect objects at different scales [27]. Next, a Region Proposal Network generates candidate Regions of Interest that are likely to contain objects [28]. To improve localization accuracy, Mask R-CNN incorporates feature alignment techniques for these Regions of Interest.

For segmentation, Mask R-CNN employs an additional mask branch to predict a binary mask for each Regions of Interest after classification and regression. This mask delineates the exact pixels corresponding to the target object. Model training is guided by a multi-task loss function that integrates classification loss, bounding box regression loss, and mask loss, thereby enabling joint optimization of detection and segmentation. Due to its excellent performance, Mask R-CNN has been widely used in

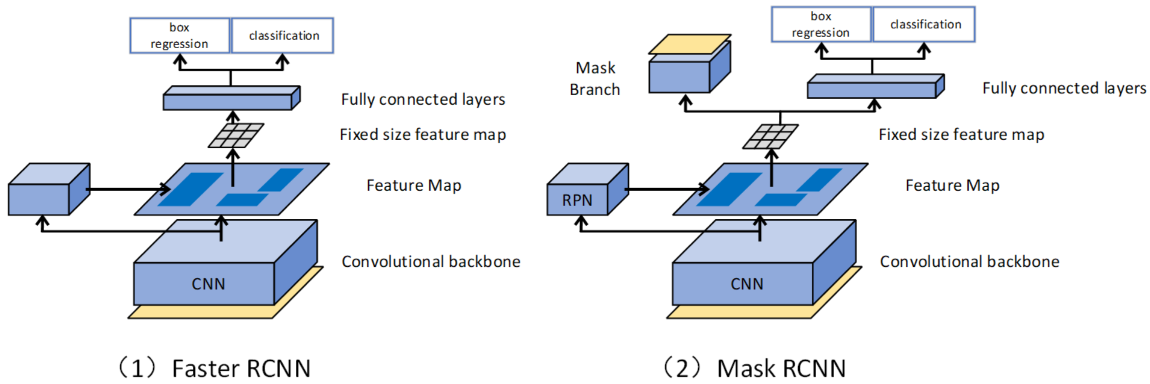

Figure 3. The fundamental architecture of R-CNNs.

autonomous driving, medical image analysis, video surveillance and other fields, providing accurate and efficient solutions for object recognition and segmentation.

Ding et al. developed a multi-objective brachial plexus segmentation network (MallesNet), derived from the Mask R-CNN framework, which achieved higher segmentation accuracy than U-Net and its variants [14]. MallesNet extends Mask R-CNN by enabling simultaneous recognition and segmentation of multiple targets. Notably, it introduces two novel modules: the Spatial Local Contrast Feature extraction module, which calculates multi-scale contrast features to effectively improve small-target recognition, and the Self-Attention Gate, which captures spatial relationships across channels and re-weights feature maps by integrating non-local operations with channel attention. In addition, the up-sampling mechanism of the original Feature Pyramid Network is improved by fine-tuning the feature map using transposed convolution and skip cascade.

U-Net

U-Net, proposed by Ronneberger et al. at the International Biomedical Imaging Challenge in 2015, has become one of the most widely used architectures for medical image segmentation [29]. Its name derives from the characteristic U-shaped structure of the network. Compared with traditional convolutional neural network, U-Net is particularly effective in delineating image boundaries and preserving fine details, thereby improving segmentation accuracy [30]. The two most important components of U-Net include the U-shaped encoder–decoder structure and the skip connection layers.

As shown in **Figure 4**, the encoder uses two consecutive convolutions to extract features and uses a 2×2 max-pooling layer to reduce the image resolution while retaining contextual information. The decoder symmetrically restores the image resolution through transposed convolution (3×3 kernels) and upsampling layers, while integrating encoder features to preserve spatial details.

The skip connection layers directly transfer feature maps from each encoder level to the corresponding decoder level. This design fuses multi-scale encoder features with corresponding decoder features, facilitating the recovery of fine-grained information during reconstruction.

Several improvements to U-Net have been proposed. For instance, Wang et al. enhanced the standard U-Net by incorporating a Recurrent Neural Network (RNN) module into the skip connections to strengthen contextual relevance [19]. Additionally, they introduced an auxiliary loss to improve the accuracy of the model. Their modified model achieved a DICE coefficient improvement of 0.08 compared with the original U-Net model.

ResNet

ResNet is a deep neural network architecture proposed by He et al. in 2015, mainly designed for image recognition and computer vision tasks [31]. In traditional deep neural networks, increasing the number of convolutional and pooling layers was assumed to improve model learning performance. However, this often leads to gradient vanishing or gradient exploding, where gradients become too small or too large, thereby hindering effective training [32]. The

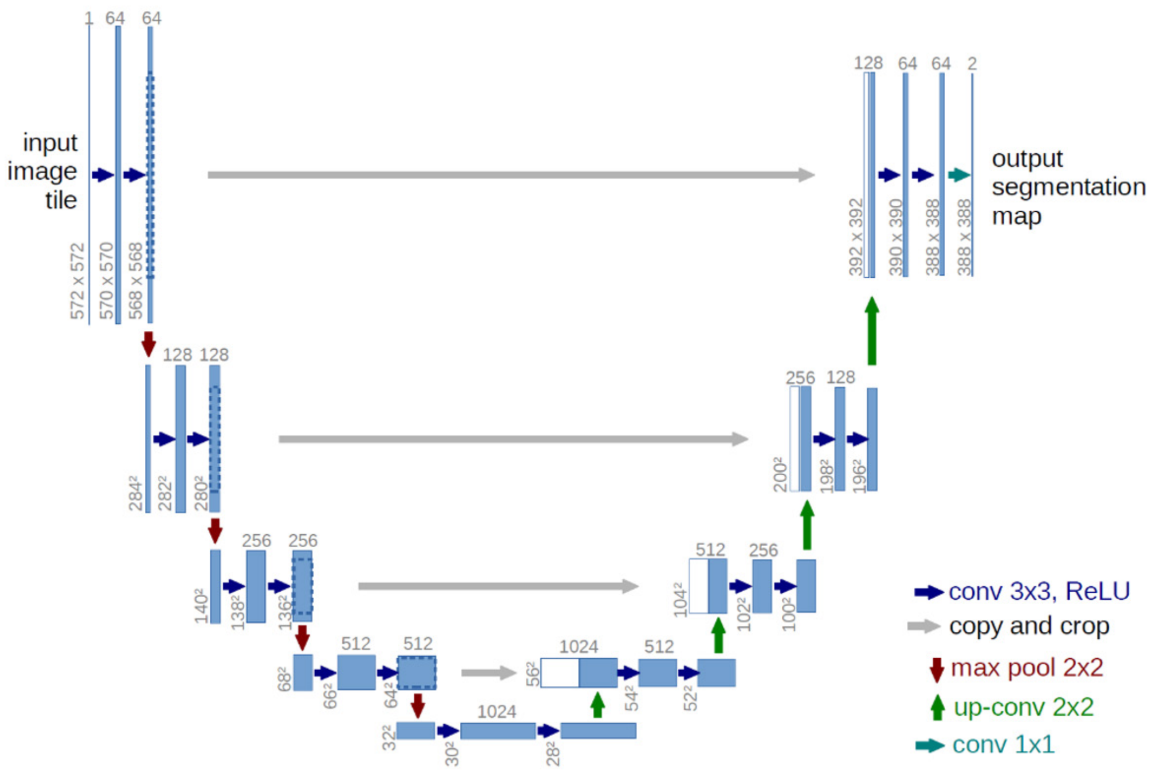

Figure 4. The fundamental architecture of U-Net. This figure was cited from [29].

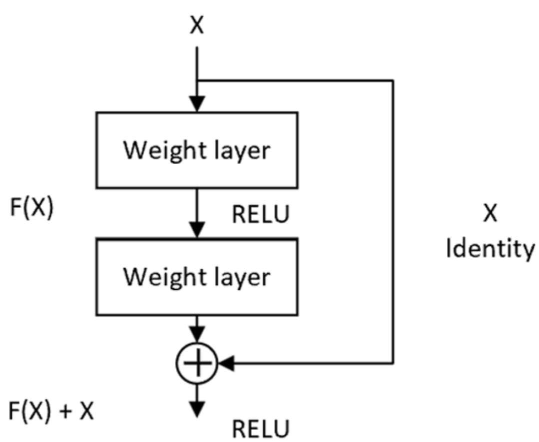

Figure 5. The fundamental architecture of ResNet. ResNet, Residual Neural Network.

core innovation of ResNet is the concept of residual learning, which solves these issues. Instead of directly mapping input to output, each layer learns the residual—the difference between the input and output. As shown in **Figure 5**, this design facilitates more efficient training and enables construction of much deeper networks capable of capturing complex features.

Wang et al. *appl*ied a ResU-Net variant for brachial plexus segmentation [20]. They first used median filtering to reduce speckle noise and then incorporated Dense Convolution and Residual Multi-kernel Pooling modules into the ResU-Net architecture. These modifications reduced spatial information loss and improved the robustness of segmentation at different scales, thereby improving segmentation accuracy. The improved model achieved a Dice coefficient of 0.649, representing an increase of 0.083 compared with the baseline ResU-Net.

Scoring criteria

In image segmentation tasks, model evaluation is essential for assessing how accurately the predicted region matches the ground truth. Since a single metric may not comprehensively capture model performance, multiple evaluation criteria are often applied in combination. Commonly used indicators include IoU or Dice coefficient.

Accuracy

Accuracy is defined as the ratio of true positives (TP) and true negatives (TN) to the total number of samples, as shown in **Table 3** [34].

$$Accuracy = \frac{TP + TN}{TP + FN + FP + TN}$$

Table 3. Confusion matrix [33]

Actual category	Predicted category	
	Positive	Negative
Positive	True Positive (TP)	False Negative (FN)
Negative	False Positive (FP)	True Negative (TN)

This measure is simple and intuitive. However, it can be misleading when the sample categories are unbalanced, as it may overestimate performance when one class dominates the dataset.

IoU

IoU evaluates the overlap between the predicted segmentation and the ground truth by calculating the ratio of their intersection to their union [35].

$$\mathrm{IoU} = \frac{TP}{FP + FN + TP}$$

IoU values range from 0 to 1, with values closer to 1 indicating higher similarity between prediction and ground truth. It provides an overall evaluation of segmentation accuracy across category.

Dice coefficient

The Dice coefficient serves as a pivotal metric for evaluating segmentation performance [36]. The goal of image segmentation is to divide an image into regions with similar features, which is usually used to identify and extract specific objects or regions in an image.

$$DICE = \frac{2\left|A \cap B\right|}{\left|A\right| + \left|B\right|}$$

Among them, A is the predicted value, and B is the true value. It compares the degree of overlap between the predicted area and the true labeled area. The Dice coefficient ranges from 0 to 1, with higher values indicating better segmentation accuracy. A Dice score of 1 denotes complete overlap, while 0 indicates no overlap at all.

Chapter summary

In recent years, a variety of deep learning models have been applied to the recognition and segmentation of brachial plexus structures in ultrasound images. Beyond conventional CNNs, models such as U-Net, ResNet, and more advanced architectures have demonstrated the ability to automatically extract image features and achieve accurate nerve segmentation. However, the inherent noise, low contrast, and complex background of ultrasound images, simple models often limit the accuracy of simple models.

To improve the accuracy of recognition and segmentation, researchers have tried to integrate specially designed modules or sub-networks into standard architectures. These modules enhance the capture of global and local context information, enabling the models to better interpret pixel-level relationships and thereby improve segmentation performance in complex imaging scenarios.

In addition, although these modifications increase the computational cost, they enhance the model's ability to manage uncertainty and fuzzy boundaries in ultrasound images. In general, inserting modules or subnetworks represents a key strategy for improving segmentation accuracy in brachial plexus ultrasound and has broad application prospects.

Existing architectures for brachial plexus segmentation

This section classifies and analyzes representative deep learning architectures for brachial plexus segmentation, as summarized in **Table 4**.

Pisda *et al.* evaluated several architectures, including fully convolutional networks, ResNet-34, and LinkNet [37-39]. Among these, LinkNet demonstrated the fastest training speed and most effective transfer learning performance on ultrasound images, with an accuracy of up to 0.8966.

Hafiane et al. briefly compared deep learning and machine learning in medical image recognition in 2017 [40]. They designed a 3-layer CNN (3×3 convolutions, Rectified Linear Unit activation, and max-pooling) that integrated spatial and temporal information. Their results showed that CNNs outperformed support vector machines, with an accuracy of 0.89 [41]. The researchers emphasized that richer data

Table 4. Performance evaluations of models for brachial plexus segmentation

Model	Reference (Year)	Database (Size)	Hardware/Software	Accuracy	Dice	IoU
FCN	Pisda *et al.* (2022)	Kaggle (9970)	NVIDIA GPU + Keras	0.8284	/	0.4800
LinkNet	Kuldeep *et al.* (2022)	Kaggle (9970)	NVIDIA GPU + Keras	0.8966	/	0.5200
CNN + spatial information	Hafiane *et al.* (2017)	Medipole Garonne Hospital (5000)	Not specified	0.8900	/	/
CNN + U-Net	Xi *et al.* (2024)	Beijing Jishuitan Hospital (502)	Not specified	/	0.7480	0.6300
MallesNet	Ding *et al.* (2022)	UBPD (1052)	NVIDIA GTX 1080Ti + TensorFlow	/	0.8460	/
U-Net	Kaggle (2016)	Kaggle (16780)	Not specified	/	0.5865	/
U-Net	Tian *et al.* (2022)	Ningbo Sixth Hospital (340)	NVIDIA GTX 1050ti/NVIDIA RTX 3090 + PyTorch	/	0.6850	/
QU-Net	Long *et al.* (2018)	Collected by themselves (11144)	NVIDIA GTX 1070 + PyTorch	0.6500	/	/
U-Net + EfficientNet	Kong *et al.* (2021)	Kaggle (5635)	NVIDIA GTX 1080 + PyTorch	/	0.7347	0.6957
U-Net + RNN	Wang *et al.* (2021)	Kaggle (5635)	Not specified	/	0.6490	/
M-Net	Abraaham *et al.* (2019)	Kaggle (5635)	NVIDIA GTX 1070 + Keras	/	0.8820	/
ResU-Net	Wang *et al.* (2019)	Kaggle (5633)	NVIDIA GTX 1080 + Keras	/	0.7093	/
YOLOv4	Sugino *et al.* (2024)	Collected by themselves (1612)	NVIDIA A100 + PyTorch	0.8150	/	/
BPMSegNet	Ding *et al.* (2020)	UBPD (1055)	NVIDIA GTX 1080Ti + TensorFlow	/	/	/
CNN+GAN	Liu *et al.* (2018)	Collected by themselves (5800)	Not specified	/	/	0.7320

Note: IoU, Intersection over Union; FCN, Fully Convolutional Network; CNN, Convolutional Neural Network; U-Net, U-shaped Network; RNN, Recurrent Neural Network; ResU-Net, Residual U-Net; GAN, Generative Adversarial Network; BPMSegNet, Brachial Plexus Multi-task Segmentation Network.

further enhance the applicability of CNNs in medical imaging.

Xi et al. trained a U-Net-based segmentation model using patient ultrasound images from Beijing Jishuitan Hospital to identify brachial plexus structures [42]. Manual annotations from experienced anesthesiologists served as the clinical gold standard for comparison. The model achieved a Dice coefficient of 0.748 and an IoU of 0.630, indicating strong overlap with expert-labeled regions. These results demonstrate the clinical potential of deep learning models in accurately and automatically identifying brachial plexus nerves.

Ding et al. enhanced Mask R-CNN by introducing a Spatial Local Contrast Feature module and a Self-Attention Gate to capture multichannel spatial relationships, and named the improved model MallesNet [14]. This model was applied not only to brachial plexus segmentation but also to the segmentation of surrounding peripheral structures such as veins, arteries, and muscles. Studies have found that leveraging these uncovered structures around the brachial plexus can facilitate the identification of brachial plexus nerves [43]. MallesNet achieved good segmentation performance on the UBPD dataset.

Tian et al. conducted a comparative study on various models for brachial plexus trunk segmentation in ultrasound images [44]. Using a dataset of 340 brachial plexus ultrasound images annotated by three experienced clinicians as the gold standard for model comparison, they evaluated 12 deep learning models and found that U-Net achieved the best segmentation accuracy with an IoU of 0.6850. Although U-Net contained only 7.76 million parameters, its processing speed was limited to 15 images per second. By contrast, LinkNet ranked second with an IoU of 0.6627 but offered higher processing efficiency, suggesting greater potential for real-time brachial plexus segmentation in the future.

Long et al. believed that the standard U-Net focuses primarily on pixel-level classification, which is insufficient to handle the high noise inherent in brachial plexus ultrasound images [45]. To address this limitation, they proposed QU-Net, incorporating a new loss function that compares pixel-level similarity between predicted and target crops. However, due to the relatively small training dataset, the accuracy rate was only 0.65.

Similarly, Kong et al. addressed the problem of blurred edges in brachial plexus images, which often leads to reduced segmentation accuracy [46]. They modified the U-Net model by incorporating dilated convolutions into the skip connections, thereby reducing noise and mitigating the imbalance between positive and negative samples. This approach achieved a Dice coefficient of 0.7347 and an IoU of 0.6957.

Wang et al. used U-Net as the basic architecture and enhanced it with a RNN module, effectively improving contextual feature extraction [19]. An auxiliary loss function was added to determine the presence or absence of brachial plexus nerves in the image, further improving model accuracy. Their findings indicated that U-Net model is efficient for capturing both global and local information, supporting its clinical applicability.

Abraham et al. tested their approach using Kaggle ultrasound dataset [47]. Differs from U-Net, their M-Net architecture has 5 convolutional layers in the encoder and utilizes average pooling rather than maximum pooling to reduce feature map resolution. Furthermore, they incorporated multi-scale decomposition, which separates signals into different frequency components: noise is primarily concentrated in small-scale (high-frequency) components, while meaningful information is distributed in large-scale (low-frequency) components. By applying thresholding and filtering, M-Net effectively suppressed high-frequency noise while preserving useful signals. Building on this principle, M-Net leverages multi-scale inputs to supervise feature maps, thereby mitigating the impact of image noise on accuracy to some extent. However, the authors noted that M-Net may suffer from overfitting and emphasized the need for larger datasets for validation.

Wang et al. observed that U-Net alone was not accurate enough in low-contrast ultrasound images [20]. To address this limitation, they integrated ResNet with U-Net and introduced Dense Convolution kernels and a Residual Multi-kernel Pooling module, realizing the ResU-Net architecture. This model achieved a Dice coefficient of 0.7093, demonstrating superior performance compared with conventional U-Net.

YOLO (You Only Look Once) is an object detection algorithm designed to achieve fast and efficient object recognition by reframing object detection as a single regression problem [48]. The model divides the image into grids, with each grid simultaneously predicting multiple bounding boxes and categories, which not only accelerates prediction efficiency but also enables detection of multiple objects within a single forward pass. The core advantage of YOLO lies in its excellent balance of speed and accuracy: compared with traditional two-stage detectors such as Faster R-CNN, YOLO greatly improves inference speed by converting the detection problem into a regression problem, while maintaining a high detection accuracy through network optimization and loss function design.

Sugino et al. applied YOLOv4 to brachial plexus ultrasound images, exploring suitable network structures and input image scales for nerve detection [49]. Using two datasets comprising 1,612 labeled brachial plexus ultrasound images, they evaluated the influence of model scaling and input size on performance. Their findings confirmed that YOLOv4's scalable architecture offers an effective trade-off between computational efficiency and segmentation accuracy, while reducing network complexity.

Against gold-standard manual annotations, the optimal model (YOLOv4-P7, 384×384 input) achieved a Dice coefficient of 0.846. Visual comparisons showed close alignment with manual labels, and real-time inference at 192.4 fps ensured practical utility.

SegNet, based on the network architecture of VGG-13, applies an unpooling structure in the decoder to enhance boundary recognition in segmentation task [50]. Ding et al. proposed a

Table 5. Performance comparison to different models on the UBPD dataset

Model	AP@mask/AP@B-box			
	AP@50	AP@60	AP@70	AP@50
Mask R-CNN	43.96/58.00	39.45/48.71	30.41/38.40	27.89/33.11
YOLACT	57.15/62.01	45.95/51.58	42.81/41.28	34.02/30.39
BPMSegNet	58.02/62.97	48.92/56.46	42.06/42.01	37.18/37.62

Note: AP, average precision; AP@50, AP@60, AP@70, precision at intersection-over-union thresholds of 0.50, 0.60, and 0.70, respectively; B-box, bounding box.

novel brachial plexus segmentation network - BPMSegNet, incorporating three key innovations: Spatial Local Contrast Features, self-attention gates, and skip connections with transposed convolutions [51]. BPMSegNet was trained and evaluated on the UBPD dataset, which they also developed, consisting of 1,055 brachial plexus ultrasound images, including nerves and surrounding tissues. For detection, BPMSegNet achieved the best results on multiple metrics, with AP@50, AP@60, AP@70 and AP reaching 62.97, 56.46, 42.01 and 37.62, respectively. In segmentation tasks, it also outperformed competing models, with the highest AP@50, AP@60 and AP scores of 58.02, 48.92 and 37.18, respectively. As shown in **Table 5**, compared with Mask R-CNN and YOLAT, BPMSegNet demonstrated segmentation results more consistent with manual annotations, with smoother edge delineation, while other models exhibited category misjudgment and missed detections [52].

Liu et al. proposed an innovative deep learning model that combines a Generative Adversarial Network (GAN) to achieve accurate segmentation of brachial plexus structure in ultrasound images [53, 54]. A GAN consists of two competing components: a generator and a discriminator. Through adversarial training, the two networks iteratively improve each other's performance, leading to more robust feature learning. The researchers pointed out two major limitations of conventional convolutional CNN-based approaches for nerve segmentation. First, CNNs may overlook subtle anatomical defects, causing suboptimal performance for pixel-level label prediction. In complex ultrasound background, this limitation reduces segmentation accuracy. Second, patient movement or inability to fully cooperate during scanning can cause the nerve region to be mistakenly identified as background, compromising the accuracy of the segmentation.

To solve the first limitation, the researchers designed a deep learning framework integrating a GAN, which consists of two main parts: a segmentation network and a discriminator network. The segmentation network aims to generate segmentation results that closely approximate the true neural structures, while the discriminator acts as a "supervisor", distinguishing between predicted outputs and ground-truth labels. Through adversarial training, the segmentation network progressively improves its performance by attempting to "fool" the discriminator into accepting its predictions as real. To address the second problem, the researchers used dilated convolution to increase the receptive field of the model. This technique allows the model to obtain more contextual information without losing resolution, thereby capturing the characteristics of neural structures over a wider range.

Experimental results demonstrated a significant improvement in segmentation accuracy. Compared with conventional FCN, the GAN-based approach increased the IoU coefficient by 27.8%, providing a more accurate and reliable solution for neural image segmentation in clinical applications. Although adversarial training did not uniformly enhance all performance metrics, it notably improved segmentation accuracy from an anatomical perspective, achieving closer consistency with manual delineation.

Discussion and challenges

Discussion

In this review, we analyzed 15 deep learning models for brachial plexus segmentation, highlighting substantial progress in this field. Early studies primarily applied simple CNNs, and subsequent research introduced more sophisticated architectures. Among them, FCN and U-Net have been intensively used due to their excellent performance. Later, numerous U-Net variants have since been proposed, often incorporating modules such as residual blocks to enhance feature learning, or adopting multi-task architectures to improve recognition capability. Overall, U-Net–based networks remain the most widely preferred for brachial plexus segmentation. The LinkNet model achieved the highest accuracy (0.8966) on the Kaggle dataset, demonstrating its strong suitability for this benchmark. M-net, proposed by Abraham *et al.* ranked second. Its deeper encoder with additional convolutional layers likely contributed to improved accuracy; however, the added complexity also raises concerns about potential overfitting, underscoring the need for larger datasets for validation.

In addition, several studies emphasized the critical role of data preprocessing [20, 55, 56]. For example, Wang et al. demonstrated that preprocessing the Kaggle dataset increased the Dice coefficient from 0.7063 to 0.7093, highlighting how appropriate preprocessing strategies can yield measurable improvements in segmentation accuracy [20].

Challenges

Despite notable progress, deep learning segmentation of brachial plexus in ultrasound imaging still faces many challenges. First, data scarcity remains the foremost issue. Publicly available datasets are limited due to patient privacy concerns, institutional data protection policies, lack of standardized annotation protocols, and the high cost of expert annotation. Consequently, many studies rely heavily on the Kaggle dataset or on restricted, unpublished data. This limitation constrains model training and hinders generalizability. Although data augmentation and image preprocessing can partially solve this problem, they cannot fundamentally overcome the upper bound imposed by insufficient data.

Furthermore, clinical translation to low-resource clinical settings is another major barrier. Characterized by—introduces additional hurdles. Real-world deployment, particularly in point-of-care scenarios (e.g., portable ultrasound machines), is constrained by limited computational power, memory capacity, and real-time inference requirements. Complex neural architectures that demand substantial GPU acceleration, high-capacity Random Access Memory (RAM), and extensive floating-point operations are often impractical for embedded systems. This challenge is compounded by the need for energy-efficient designs to prevent overheating in portable devices, further restricting model complexity. These challenges not only affect the practicality of the model but also raise important questions about future research directions and technological development.

Looking forward, future research must focus on enhancing model generalization under limited data conditions and identify the best optimization strategy to advance the clinical applicability of deep learning for brachial plexus ultrasound imaging.

Future research directions

As highlighted in the preceding discussion, there is a significant shortage of publicly available brachial plexus datasets, particularly in ultrasound imaging. Therefore, establishing a comprehensive, standardized, and expert-annotated public dataset is of critical importance. As the volume and quality of training data increase, the performance and generalizability of deep learning models are expected to improve substantially, thereby accelerating progress in this research area.

To address this challenge, efforts should be directed at both policy and technical fronts. From a policy perspective, data-sharing agreements and multi-institutional collaborations should be encouraged, supported by ethical frameworks and regulatory guidelines. From a technical perspective, privacy-preserving strategies such as data encryption, federated learning, and differential privacy offer secure solutions for cross-institutional data utilization without compromising patient confidentiality. Collectively, these strategies will enable the development of high-quality datasets and robust models, ultimately enhancing the clinical applicability of deep learning in brachial plexus ultrasound segmentation.

Another important research direction involves improving the practical deployability of deep learning models in real-world clinical environments. While many models demonstrate excellent segmentation accuracy under controlled settings, their high computational requirements often hinder application in low-resource or point-of-care scenarios. Future studies should focus on optimizing existing algorithms or developing lightweight, efficient architectures capable of supporting real-time segmentation on embedded or portable ultrasound devices. Techniques such as model pruning, quantization, and knowledge distillation can reduce model size and computational cost while preserving accuracy. Moreover, integrating optimized models with ultrasound systems through interoperable software interfaces or plug-in modules will be essential for seamless clinical adoption. Exploring on-device inference, edge computing, and low-latency processing pipelines will further facilitate the development of lightweight, hardware-friendly AI tools that support real-time decision-making, reduce clinician workload, and enhance diagnostic efficiency.

In this context, combining high-quality datasets with optimized algorithms will not only improve segmentation accuracy in brachial plexus ultrasound imaging but also advance the broader field of medical imaging. Such innovations have the potential to streamline clinical workflows and improve patient care outcomes.

Meanwhile, most current studies on brachial plexus segmentation emphasize performance metrics such as Dice and IoU, while few address the interpretability of deep learning models. In clinical scenarios, however, explainability is crucial for building trust among healthcare providers. Future work should consider incorporating interpretability techniques such as Gradient-weighted Class Activation Mapping, which generates visual heatmaps to highlight the most influential regions in the input image, thereby clarifying the model's decision-making process. Similarly, the application of attention mechanisms can provide insight into feature importance during segmentation. These approaches can significantly enhance the clinical acceptance of AI tools in ultrasound-guided procedures.

Conclusion

This review summarizes recent progress in applying deep learning to brachial plexus ultrasound image segmentation, including the availability of public datasets, commonly used segmentation models, and their evaluation metrics. The main contribution of this review is to analyze existing models, highlight emerging trends, and outline future research directions in this field. These insights may assist researchers in developing accurate, robust, and clinically applicable models for ultrasound-guided brachial plexus segmentation.

Author contributions: Jiaen Wu: Responsible for the primary research work of the paper, including literature review, data analysis, and writing the article. Miao Zhou: Responsible for part of the literature review and writing of specific chapters, particularly those related to relevant work and background. Zhaopeng Zhou, Jiaxun Jiang: Participated in data collection and organization, contributing to the discussion of technical details and methods. Jinjing Wu: Participated in the revision and organization of the paper, mainly helping with formatting and language. Haipo Cui: Corresponding Author: Responsible for the overall conception and review of the paper, guiding the research direction, and finalizing and revising the paper.

References

[1] Grzeczka A, Skowroński A, Zdun M. Anatomy of the brachial plexus (Plexus brachialis) and innervation of the thoracic limb of the Caracal (Caracal caracal). Medical Journal of Cell Biology 2024;12(3):107-116.

[2] Hems T. Chapter 44 - Brachial Plexus Injuries. In: Tubbs RS, Rizk E, Shoja MM, et al., editors. Nerves and Nerve Injuries. San Diego. Academic Press, 2015. p. 681-706.

[3] Lovaglio AC, Socolovsky M, Di Masi G, et al. Treatment of neuropathic pain after peripheral nerve and brachial plexus traumatic injury. Neurol India 2019;67(Supplement):S32-S37.

[4] Goldsmith AJ, Brown J, Duggan NM, et al. Ultrasound-guided nerve blocks in emergency medicine practice: 2022 updates. Am J Emerg Med 2024;78:112-119.

[5] Niyonkuru E, Iqbal MA, Zeng R, et al. Nerve Blocks for Post-Surgical Pain Management: A Narrative Review of Current Research. J Pain Res 2024;17:3217-3239.

[6] Zhang L, Pang R, Zhang L. Comparison of ultrasound-guided costoclavicular and supraclavicular brachial plexus block for upper extremity surgery: a propensity score matched retrospective cohort study. Ann Palliat Med 2021;10(1): 454-461.

[7] Prajapati N, Chauhan MAZ, Chaudhary D, et al. Efficacy of ultrasound guided peripheral nerve blocks versus conventional methods in regional Anesthesia. Int J Life Sci, Biotechnol Pharm Res 2025;14(1):342-345.

[8] Warman P, Nicholls B. Ultrasound-guided nerve blocks: efficacy and safety. Best Pract Res Clin Anaesthesiol 2009;23(3):313-326.

[9] Liu S, Wang Y, Yang X, et al. Deep Learning in Medical Ultrasound Analysis: A Review. Engineering 2019;5(2):261-275.

[10] Zhang A, Lipton ZC, Li M, et al. Dive into Deep Learning. arXiv 2021;arXiv:2106.11342.

[11] Zhao H, Sun N. Improved U-Net Model for Nerve Segmentation. Image and Graphics. ICIG 2017. Lecture Notes in Computer Science 2017;496-504.

[12] Yan S, Chen X, Tang X, et al. Segmentation of Brachial Plexus Ultrasound Images Based on Modified SegNet Model. Intelligent Data Engineering and Automated Learning – IDEAL 2023 2023;332-344.

[13] Ultrasound Nerve Segmentation. Available at: https://www.kaggle.com/competitions/ultrasound-nerve-segmentation

[14] Ding Y, Yang Q, Wang Y, et al. MallesNet: A multi-object assistance based network for brachial plexus segmentation in ultrasound images. Med Image Anal 2022;80:102511.

[15] Cao W, Howe BM, Wright DE, et al. Abnormal Brachial Plexus Differentiation from Routine Magnetic Resonance Imaging: An AI-based Approach. Neuroscience 2024;546:178-187.

[16] Burger W, Burge M. Digital Image Processing: An Algorithmic Introduction. Springer Cham, 2022.

[17] Bieniecki W, Grabowski S, Rozenberg W. Image Preprocessing for Improving OCR Accuracy. 2007 International Conference on Perspective Technologies and Methods in MEMS Design 2007;75-80.

[18] Lv YC, Jiang Q, Xu YH, et al. Improved brachial plexus nerve segmentation method based on multi-scale feature fusion. J Comput Appl 2023;43(01):273-279.

[19] Wang Y, Geng J, Zhou C, et al. Segmentation of Ultrasound Brachial Plexus Based on U-Net. 2021 International Conference on Communications, Information System and Computer Engineering (CISCE) 2021;482-485.

[20] Wang R, Shen H, Zhou M. Ultrasound Nerve Segmentation of Brachial Plexus Based on Optimized ResU-Net. 2019 IEEE International Conference on Imaging Systems and Techniques (IST) 2019;1-6.

[21] Alzubaidi L, Zhang J, Humaidi AJ, et al. Review of deep learning: concepts, CNN architectures, challenges, applications, future directions. J Big Data 2021;8(1):53.

[22] Agarap AF. Deep Learning using Rectified Linear Units (ReLU). arXiv 2018;arXiv:1803.08375.

[23] Verdhan V. Image classification using LeNet. Computer vision Using Deep learning: Neural Network Architectures with Python and Keras. New York (USA). Apress Berkeley, CA, 2021. p. 67-101.

[24] Szegedy C, Wei L, Yangqing J, et al. Going deeper with convolutions. 2015 IEEE Conference on Computer Vision and Pattern Recognition (CVPR) 2015;1-9.

[25] Boxtel JV, Vousten V, Pluim J, et al. Hybrid Deep Neural Network for Brachial Plexus Nerve Segmentation in Ultrasound Images. 2021 29th European Signal Processing Conference (EUSIPCO) 2021;1246-1250.

[26] He K, Gkioxari G, Dollár P, et al. Mask R-CNN. 2017 IEEE International Conference on Computer Vision (ICCV) 2017;2980-2988.

[27] Lin TY, Dollár P, Girshick R, et al. Feature Pyramid Networks for Object Detection. 2017 IEEE Conference on Computer Vision and Pattern Recognition (CVPR) 2017;936-944.

[28] Ren S, He K, Girshick R, et al. Faster R-CNN: Towards Real-Time Object Detection with Region Proposal Networks. IEEE Trans Pattern Anal Mach Intell 2017;39(6):1137-1149.

[29] Ronneberger O, Fischer P, Brox T. U-Net: Convolutional Networks for Biomedical Image Segmentation. Medical Image Computing and Computer-Assisted Intervention – MICCAI 2015 2015;234-241.

[30] Siddique N, Paheding S, Elkin CP, et al. U-Net and Its Variants for Medical Image Segmentation: A Review of Theory and Applications. IEEE Access 2021;9:82031-82057.

[31] He K, Zhang X, Ren S, et al. Deep Residual Learning for Image Recognition. 2016 IEEE Conference on Computer Vision and Pattern Recognition (CVPR) 2016;770-778.

[32] Hanin B. Which neural net architectures give rise to exploding and vanishing gradients? arXiv 2018;arXiv:1801.03744.

[33] Caelen O. A Bayesian interpretation of the confusion matrix. Ann Math Artif Intel 2017;81(3):429-450.

[34] Tharwat A. Classification assessment methods. Appl Comput Inform 2020;17(1):168-192.

[35] Cho YJ. Weighted Intersection over Union (wIoU) for evaluating image segmentation. Pattern Recognit Lett 2024;185:101-107.

[36] Eelbode T, Bertels J, Berman M, et al. Optimization for Medical Image Segmentation: Theory and Practice When Evaluating With Dice Score or Jaccard Index. IEEE Trans Med Imaging 2020;39(11):3679-3690.

[37] Pisda K, Jain P, Sisodia DS. Deep Networks for Brachial Plexus Nerves Segmentation and Detection Using Ultrasound Images. Information Systems and Management Science 2021;132-146.
[38] Koonce B. ResNet50. Convolutional neural networks with swift for tensorflow: image recognition and dataset categorization. Apress Berkeley, CA, 2021. p. 63-72.
[39] Chaurasia A, Culurciello E. LinkNet: Exploiting encoder representations for efficient semantic segmentation. 2017 IEEE Visual Communications and Image Processing (VCIP) 2017;1-4.
[40] Hafiane A, Vieyres P, Delbos A. Deep learning with spatiotemporal consistency for nerve segmentation in ultrasound images. arXiv 2017;arXiv:1706.05870.
[41] Pisner DA, Schnyer DM. Chapter 6 - Support vector machine. In: Mechelli A, Vieira S, editors. Machine Learning. Academic Press, 2020. p. 101-121.
[42] Xi Y, Chong H, Zhou Y, et al. Convolutional neural network for brachial plexus segmentation at the interscalene level. BMC Anesthesiol 2024;24(1):17.
[43] Ustuner E, Yılmaz A, Özgencil E, et al. Ultrasound anatomy of the brachial plexus nerves in the neurovascular bundle at the axilla in patients undergoing upper-extremity block anesthesia. Skeletal Radiol 2013;42(5):707-713.
[44] Tian D, Zhu B, Wang J, et al. Brachial Plexus Nerve Trunk Recognition From Ultrasound Images: A Comparative Study of Deep Learning Models. IEEE Access 2022;10:82003-82014.
[45] Long FN, Zhu XS, Gan JZ. Ultrasound Image Segmentation of Brachial Plexus via Convolutional Neural Networks. J Hefei Univ Technol 2018;41(09):1191-1195+1296.
[46] Kong LJ, Wang QW, Bao YC, et al. A Brachial Plexus Ultrasound Image Segmentation Network Based on Deep Learning. Radio Eng 2021;51(09):841-847.
[47] Abraham N, Illanko K, Khan N, et al. Deep Learning for Semantic Segmentation of Brachial Plexus Nervesin Ultrasound Images Using U-Net and M-Net. 2019 3rd International Conference on Imaging, Signal Processing and Communication (ICISPC) 2019;85-89.
[48] Jiang P, Ergu D, Liu F, et al. A Review of Yolo Algorithm Developments. Procedia Comput Sci 2022;199:1066-1073.
[49] Sugino T, Onogi S, Oishi R, et al. Investigation of Appropriate Scaling of Networks and Images for Convolutional Neural Network-Based Nerve Detection in Ultrasound-Guided Nerve Blocks. Sensors (Basel) 2024;24(11):3696.
[50] Badrinarayanan V, Kendall A, Cipolla R. SegNet: A Deep Convolutional Encoder-Decoder Architecture for Image Segmentation. IEEE Trans Pattern Anal Mach Intell 2017;39(12):2481-2495.
[51] Ding Y, Yang Q, Wu G, et al. Multiple Instance Segmentation in Brachial Plexus Ultrasound Image Using BPMSegNet. arXiv 2020;arXiv:2012.12012.
[52] Jiang X, Liu L, Shan C, et al. Recognizing vector graphics without rasterization. arXiv 2021;arXiv:2111.03281.
[53] Liu C, Liu F, Wang L, et al. SEGMENTATION OF NERVE ON ULTRASOUND IMAGES USING DEEP ADVERSARIAL NETWORK. International Journal of Innovative Computing, Information and Control 2018;14(1):53-64.
[54] Goodfellow I, Pouget-Abadie J, Mirza M, et al. Generative adversarial networks. arXiv 2020; arXiv:1406.2661.
[55] Vashishtha V, Aju D. Nerve segmentation in ultrasound images. 2017 Innovations in Power and Advanced Computing Technologies (i-PACT) 2017;1-5.
[56] Wang Y, Zhu B, Kong L, et al. Brachial Plexus Nerve Trunk Segmentation Using Deep Learning: A Comparative Study with Doctors' Manual Segmentation. arXiv 2022;arXiv: 2205.08143.